Determination of Local Ligand Conformations in Slowly Tumbling Proteins by Homonuclear 2D and 3D NMR: Application to Heme Propionates in Leghemoglobin

Dimitrios Morikis, Rafael Brüschweiler, and Peter E. Wright*

Contribution from the Department of Molecular Biology, The Scripps Research Institute, 10666 North Torrey Pines Road, La Jolla, California 92037

Received January 19, 1993

Abstract: A novel procedure for proton assignment and determination of the conformation of the heme propionates of heme proteins is described. Analysis of 3D TOCSY–NOESY and NOESY–NOESY NMR spectra of carbonmonoxy leghemoglobin (LbCO) allowed the unambiguous identification of the spin systems of both heme propionates. Long-range ROE-type transfers observed in 3D TOCSY–NOESY and 2D TOCSY spectra have been found to be useful for identifying the heme propionate protons. NOE buildup curves have been measured and provide evidence for spin diffusion at mixing times less than 50 ms. Cross-peak volumes and J coupling information extracted from a 30-ms 2D NOESY and a 2QF-COSY spectrum, respectively, have been used for the determination of the propionate assignments and conformations. For both propionates, an independent grid search about two rotatable torsion angles performed with a 10° increment allowed sampling of 1296 different conformations. Intra-heme NOE cross-relaxation rates and ^3J coupling constants have been back-calculated for each of these conformations by taking into account all possible assignments, including stereospecific assignments, and compared with the experimental data. Additional NOEs to the globin allow discrimination between propionate mirror images with respect to the heme plane. Conformations were obtained that are a good fit to the experimental data, providing unambiguous (stereo) assignments for the propionate methylene proton resonances. The propionate conformations determined by NMR are compared with those found in crystal structures of lupin leghemoglobin (Lb) and other heme proteins. Possible hydrogen-bonding interactions involving the propionate carboxyl groups and globin side chains are discussed. This study demonstrates the possibility of detailed local structural characterization of a ligand embedded in a slowly tumbling protein by homonuclear NMR using only limited qualitative distance information to the protein.

1. Introduction

Myoglobin (Mb) and hemoglobin (Hb) are among the best studied heme proteins. They contain the prosthetic group iron protoporphyrin IX (Figure 1) which carries two symmetrically placed propionate groups, two asymmetrically placed vinyl groups, and four methyl groups. The exact role of the heme propionates in correctly orienting the heme and in binding ligands is not yet fully understood and has been the subject of several investigations.[1] Interactions of the heme propionate groups with the polypeptide side chains, through salt bridges and steric effects, have been proposed to stabilize the heme within the heme pocket.[1a,b,2] Although it has been argued previously that the vinyl contacts are more important than propionate contacts in determining the equilibrium orientation of the heme in sperm whale Mb following reconstitution,[1a,c] it has been suggested that the initial heme-protein complex is due to the formation of a salt bridge between 6-propionate[3] and arginine 45 (CD3).[1d]

A number of structures of heme proteins have been obtained using diffraction techniques, providing additional information on the propionates.[4] The X-ray structures of sperm whale metMb[4a] and carbonmonoxy Mb (MbCO)[4b] and the neutron diffraction structure of MbCO[4c] indicate hydrogen bonding between the 6-propionate and the side chain of arginine 45 and between the 7-propionate and the ring of histidine 97 (FG3). The X-ray structure of MbCO suggests that the side chain of arginine 45 is present in two equally populated conformations.[4b] A functional role for the mobility of arginine 45 was proposed,[4b] facilitating the ligand entry into the heme pocket in a concerted motion with the distal histidine. Although similar disorder for arginine 45 is not discussed in the neutron diffraction study of MbCO,[4c] the authors agree that the complex hydrogen-bonding network of arginine 45 might control ligand affinity; however, it has been argued, on the basis of kinetic data on site-directed mutants of Mb, that residue 45 regulates oxygen affinity to a far lesser extent than the distal histidine (His64, E7).[5] The X-ray structure of horse heart metMb[4d] also indicates salt bridges between 6-propionate and lysine 45 (CD3) and between 7-pro-

* Author to whom correspondence should be addressed.

(1) (a) Hauksson, J. B.; La Mar, G. N.; Pandey, R. K.; Rezzano, I. N.; Smith, K. M. *J. Am. Chem. Soc.* **1990**, *112*, 6198–6205. (b) La Mar, G. N.; Hauksson, J. B.; Dugad, L. B.; Liddel, P. A.; Venkataramana, N.; Smith, K. M. *J. Am. Chem. Soc.* **1991**, *113*, 1544–1550. (c) La Mar, G. N.; Emerson, S. D.; Lecomte, J. T. J.; Pande, U.; Smith, K. M.; Craig, G. W.; Kehres, L. A. *J. Am. Chem. Soc.* **1986**, *108*, 5568–5573. (d) La Mar, G. N.; Pande, U.; Hauksson, J. B.; Pandey, R. K.; Smith, K. M. *J. Am. Chem. Soc.* **1989**, *111*, 485–491.

(2) (a) Neya, S.; Funasaki, N. *J. Biol. Chem.* **1987**, *262*, 6725–6728. (b) Neya, S.; Funasaki, N. *Biochim. Biophys. Acta* **1988**, *952*, 150–157.

(3) The 6- and 7-propionates are attached to pyrrole rings III and IV, respectively.

(4) (a) Takano, T. *J. Mol. Biol.* **1977**, *110*, 537–568. (b) Kuriyan, J.; Wilz, S.; Karplus, M.; Petsko, G. A. *J. Mol. Biol.* **1986**, *192*, 133–154. (c) Cheng, X.; Schoenborn, B. P. *J. Mol. Biol.* **1991**, *220*, 381–399. (d) Evans, S. V.; Brayer, G. D. *J. Mol. Biol.* **1990**, *213*, 885–897. (e) Bolognesi, M.; Onesti, S.; Gatti, G.; Coda, A.; Ascenzi, P.; Brunori, M. *J. Mol. Biol.* **1989**, *205*, 529–544. (f) Arutyunyan, E. G.; Kuranova, I. P.; Vainshtein, B. K.; Steigemann, W. *Sov. Phys. Crystallogr. (Engl. Transl.)* **1980**, *25*, 43–58 and references therein. (g) Arutyunyan, E. G. *Mol. Biol. (Engl. Trans.)* **1981**, *15*, 19–33 and references therein. (h) Arutyunyan, E. G.; Deisenhofer, J.; Templyakov, A. V.; Kuranova, G. V.; Obmolova, G. V.; Vainshtein, B. K. *Dokl. Akad. Nauk (SSSR) (Engl. Transl.)* **1983**, *270*, 732–736. (i) Ollis, D. L.; Appleby, C. A.; Colman, P. M.; Cutten, A. E.; Guss, J. M.; Venkatappa, M. P.; Freeman, H. C. *Aust. J. Chem.* **1983**, *36*, 451–468. (j) Phillips, S. E. V. *J. Mol. Biol.* **1980**, *142*, 531–554. (k) Takano, T. *J. Mol. Biol.* **1977**, *110*, 569–584. (l) Lionetti, C.; Guanziroli, M. G.; Frigerio, F.; Ascenzi, P.; Bolognesi, M. *J. Mol. Biol.* **1991**, *217*, 409–412. (m) Phillips, G. N., Jr.; Arduini, R. M.; Springer, B. A.; Sligar, S. G. *Proteins: Struct., Funct. Genet.* **1990**, *7*, 358–365. (n) Arents, G.; Love, W. E. *J. Mol. Biol.* **1989**, *210*, 149–161. (o) Steigemann, W.; Weber, E. *J. Mol. Biol.* **1979**, *127*, 309–338. (p) Fermi, G.; Perutz, M. F.; Shaanan, B.; Fourme, R. *J. Mol. Biol.* **1984**, *175*, 159–174. (q) Baldwin, J. M. *J. Mol. Biol.* **1980**, *136*, 103–128. (r) Shaanan, B. *J. Mol. Biol.* **1983**, *171*, 31–59. (s) Takano, T.; Dickerson, R. E. *J. Mol. Biol.* **1981**, *153*, 79–94. (t) Takano, T.; Dickerson, R. E. *J. Mol. Biol.* **1981**, *153*, 95–115.

0002-7863/93/1515-6238$04.00/0

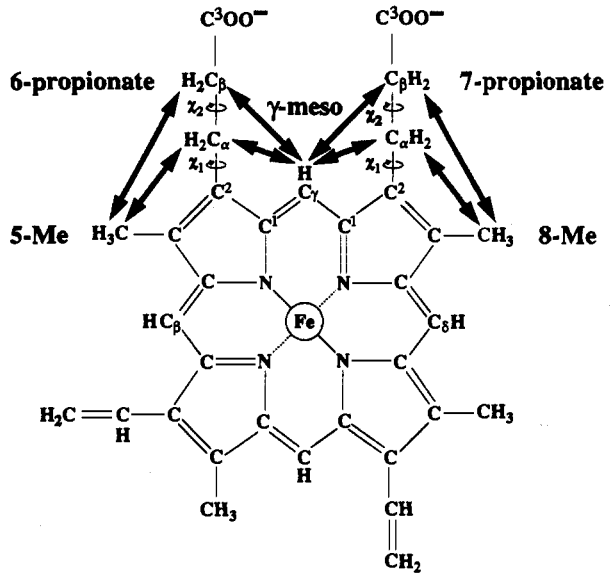

Figure 1. Schematic representation of the heme outlining the assignment strategy. The arrows connect pairs of protons involved in the NOE cross-peaks used for assignments. The nomenclature used in the text is also shown. The χ_1 and χ_2 torsion angles mentioned in the text are defined by the carbon atoms labeled as $C^1C^2C_\alpha C_\beta$ and $C^2C_\alpha C_\beta C^3$, respectively. The zero positions of the torsion angles are defined as follows: $\chi_1 = 0°$ for C^1–C^2 cis to C_α–C_β and $\chi_2 = 0°$ for C^2–C_α cis to C_β–C^3. The rotation direction for χ_1 is positive when the viewer is located on the C^2 atom and observes a clockwise rotation around the C^2–C_α bond. A similar definition applies for χ_2 when the viewer is located on the C_α atom and observes a clockwise rotation about the C_α–C_β bond. A $\chi_1 = 90°$ will rotate the 6- and 7-propionate side chains toward the distal and proximal sides of the heme, respectively.

pionate and histidine 97 (FG3). It has been suggested that the link between 6-propionate and residue 45 is weaker in horse Mb than in sperm whale Mb,[1a] and the different proton-exchange behavior of the two proteins has been attributed to the difference in the stabilities of the 6-propionate–lysine and –arginine 45 salt bridges, respectively.[6]

In contrast to sperm whale and horse Mb, ferric *Aplysia limacina* Mb lacks salt bridges between the propionate chains and the globin.[4e] The same X-ray structure suggests conformational disorder and high mobility for 7-propionate and a single conformation for 6-propionate. Conformational disorder for heme substituents was also recently demonstrated for the vinyl groups of metcyano Mb (MbCN).[7] The X-ray structure of lupin ferric acetate leghemoglobin (Lb) suggests hydrogen bonding to serine 45 (CD2) for 6-propionate and hydrogen bonds to solvent molecules, but not to the protein, for 7-propionate.[4f-h] The 3.3-Å low-resolution structure of soybean ferric nicotinate Lb is not sufficient to yield orientations for the propionates.[4i]

In the present study, we focus on the solution conformation of the heme propionates of soybean carbonmonoxy leghemoglobin (LbCO). NMR provides local information about inter-proton distances and torsion angles, allowing a direct comparison with X-ray structures of homologous proteins. Since no 3D structure is available yet for soybean LbCO, an attempt is made to determine the propionate conformations mainly on the basis of intra-heme NOEs and a limited number of heme-protein NOEs. In this sense, this work is a pilot study on the potential of NMR to investigate local conformational features in a slowly tumbling biomolecule, ignoring to a large extent more global structural information. For the first step, described in section 3, identification of the propionate spin systems is made using homonuclear 3D NMR.[8] This overcomes the need for utilization of hyperfine shifts induced by a paramagnetic heme iron atom to make the propionate assignments[1] and allows us to work directly with the functionally more important diamagnetic complexes. In section 4, a grid search is described in the conformation space spanned by the two rotatable propionate torsion angles. From the modeled conformations, taking into account all possible assignments (including stereospecific assignments), NOESY and *J* coupling data are back-calculated and compared with the experimental data in order to identify the best-fitting assignment and conformation. In section 5, the results are compared with other NMR and X-ray studies on homologous systems.

A procedure for obtaining stereospecific assignments in the course of structure determination has been introduced first using distance geometry calculations.[9] The method described in the present paper works directly in torsion angle space and is similar to a procedure described by Güntert *et al.*[10] The two main differences are that here quantitative cross-peak volumes are used rather than qualitative cross-peak intensities as in ref 10 and that, in the present work, not only changes in stereospecific assignments but also changes in real proton assignments involving a change of the directly bonded carbon atoms are allowed.

2. Materials and Methods

Carbonmonoxy leghemoglobin a samples were prepared in potassium phosphate buffer 0.05 M in 90% H_2O/10% D_2O, pH 7, using methods described elsewhere.[11] All NMR data were collected on a Bruker AMX-600 spectrometer at 308 K.

A homonuclear 3D TOCSY–NOESY spectrum[8f] with a TOCSY mixing time of 60 ms and a NOESY mixing time of 175 ms, respectively, was recorded with $256(t_1) \times 156(t_2) \times 2048(t_3)$ real data points. A homonuclear 3D NOESY–NOESY spectrum[8g] with both NOE mixing times set to 100 ms was recorded with $256(t_1) \times 124(t_2) \times 2048(t_3)$ real data points. For both TOCSY–NOESY and NOESY–NOESY, the spectral widths were set to 12.5 kHz in the t_3 dimension and to 8.5 kHz in t_1 and t_2. The spectra were collected with time-proportional phase incrementation (TPPI)[12a] in both t_1 and t_2 dimensions. The recycling delay was 1.2 s for the TOCSY–NOESY and 1.5 s for the NOESY–NOESY spectrum, during which weak water saturation was applied. In both pulse sequences a Hahn echo[12b] was utilized prior to acquisition in order to reduce baseline distortion and to circumvent first-order phase error along ω_3. The first t_3 point was generated with linear prediction. In order to avoid first-order phase correction along t_1 and t_2, the data were collected with sine modulation[12c] in these dimensions and the first point was either back-predicted or set to zero during processing. For spectral processing, a 90°-shifted sine bell window function was applied in t_3 and the Kaiser window function with $\theta = \pi$ was used in both t_1 and t_2 dimensions, respectively. Linear baseline correction was applied in ω_3 after Fourier transformation and phase correction. Zero-filling in t_1 and t_2 dimensions followed by Fourier transformation yielded real matrices of size $256(\omega_1) \times 256(\omega_2) \times 1024(\omega_3)$.

An NOE buildup series was collected using standard 2D NOESY spectra,[12d] recorded with mixing times of 30, 50, 75, 100, and 200 ms.

(5) Carver, T. E.; Olson, J. S.; Smerdon, S. J.; Krzywda, S.; Wilkinson, A. J.; Gibson, Q. H.; Blackmore, R. S.; Dezz Ropp, J.; Sligar, S. G. *Biochemistry* **1991**, *30*, 4697–4705.

(6) Lecomte, J. T. J.; La Mar, G. N. *Biochemistry* **1985**, *24*, 7388–7395.

(7) Yamamoto, Y.; Iwafune, K.; Nanai, N.; Chujo, R.; Inoue, Y.; Suzuki, T. *Biochim. Biophys. Acta* **1992**, *1120*, 173–182.

(8) (a) Griesinger, C.; Sørensen, O. W.; Ernst, R. R. *J. Am. Chem. Soc.* **1987**, *109*, 7227–7228. (b) Griesinger, C.; Sørensen, O. W.; Ernst, R. R. *J. Magn. Reson.* **1987**, *73*, 574–579. (c) Oschkinat, H.; Griesinger, C.; Kraulis, P. J.; Sørensen, O. W.; Ernst, R. R.; Gronenborn, A. M.; Clore, G. M. *Nature* **1988**, *332*, 374–376. (d) Vuister, G. W.; Boelens, R.; Kaptein, R. *J. Magn. Reson.* **1988**, *80*, 176–185. (e) Griesinger, C.; Sørensen, O. W.; Ernst, R. R. *J. Magn. Reson.* **1989**, *84*, 14–63. (f) Oschkinat, H.; Cieslar, C.; Gronenborn, A. M.; Clore, G. M. *J. Magn. Reson.* **1989**, *81*, 212–216. (g) Boelens, R.; Vuister, G. W.; Koning, T. M. G.; Kaptein, R. *J. Am. Chem. Soc.* **1989**, *111*, 8525–8526. (h) Simorre, J.-P.; Marion, D. *J. Magn. Reson.* **1991**, *94*, 426–432.

(9) Weber, P. L.; Morrison, R.; Hare, D. *J. Mol. Biol.* **1988**, *204*, 483–487.

(10) Güntert, P.; Braun, W.; Billeter, M.; Wüthrich, K. *J. Am. Chem. Soc.* **1989**, *111*, 3997–4004.

(11) Morikis, D.; Lepre, C. A.; Wright, P. E. Manuscript in preparation.

(12) (a) Marion, D.; Wüthrich, K. *Biochem. Biophys. Res. Commun.* **1983**, *113*, 967–974. (b) Rance, M.; Byrd, R. A. *J. Magn. Reson.* **1983**, *52*, 221–240. (c) Marion, D.; Bax, A. *J. Magn. Reson.* **1988**, *79*, 352–356. (d) Macura, S.; Huang, Y.; Suter, D.; Ernst, R. R. *J. Magn. Reson.* **1981**, *43*, 259–281. (e) Rance, M.; Sørensen, O. W.; Bodenhausen, G.; Wagner, G.; Ernst, R. R.; Wüthrich, K. *Biochem. Biophys. Res. Commun.* **1983**, *117*, 479–485.

All other spectral acquisition and processing parameters were similar to those used for the 3D spectra except for the use of Lorentz to Gauss transformation and shifted sine bell window functions in t_2 and t_1, respectively. For the 2D 2QF-COSY spectrum,[12e] acquisition and processing parameters were similar to those for the 2D NOESY and the 3D spectra but without sine modulation in t_1.

Spectral processing, NOE volume integration, and data-base bookkeeping were done using the software FELIX.[13] Torsion angles for Table IV were extracted from X-ray structure coordinates deposited in the Brookhaven Protein Data Bank (PDB)[14] using the software package SYBYL.[15] The heme propionate conformations for the grid search were generated using the molecular mechanics program CHARMM.[16]

3. Spin System Identification

In recent years, a series of ^{1}H NMR studies of diamagnetic heme proteins that contain protoporphyrin IX prosthetic groups have been reported. Some of these studies were aimed toward structure determination of heme proteins and include proton assignments of the heme.[17,18] Although the heme methyl and vinyl substituents and the meso protons are easy to assign, in only a few studies have partial or complete assignments of the two heme propionates been achieved.[18] Proton resonances of the heme propionates are often difficult to assign using conventional 1D and 2D ^{1}H NMR for a number of reasons: (a) severe overlap with other protein backbone and side chain protons, (b) the proximity of some propionate proton resonances to the water resonance leading to intensity attenuation when solvent suppression is applied, (c) incomplete TOCSY transfers within the propionate spin systems, and (d) rather large line widths that cause cancellation of the antiphase multiplet components in 2Q or COSY spectra. Comparison of the ^{1}H resonances of the protein-bound porphyrins to those of free porphyrins assigned earlier[19] yields only partial assignments of the propionates since the removal of the degeneracy of the two α and the two β protons in the presence of the globin introduces the need for stereospecific assignments.

In the present study, a new procedure is used for heme propionate spin system identification, using homonuclear 3D TOCSY–NOESY and NOESY–NOESY spectra.[8] Unlike heteronuclear 3D NMR,[20] homonuclear 3D spectroscopy does not benefit from efficient magnetization transfers via large ^1J couplings and improved chemical shift dispersion; however, it is, when labeled proteins are not available, very useful for overcoming practical limitations of 2D NMR applied to larger proteins. As in heteronuclear 3D experiments, the higher dimensionality increases the spectral resolution at the cost of lower digital resolution and somewhat lower sensitivity. The occurrence of two successive magnetization transfers involving up to three protons yields a large number of additional cross-peaks in the ^{1}H 3D spectra when compared to conventional 2D or heteronuclear

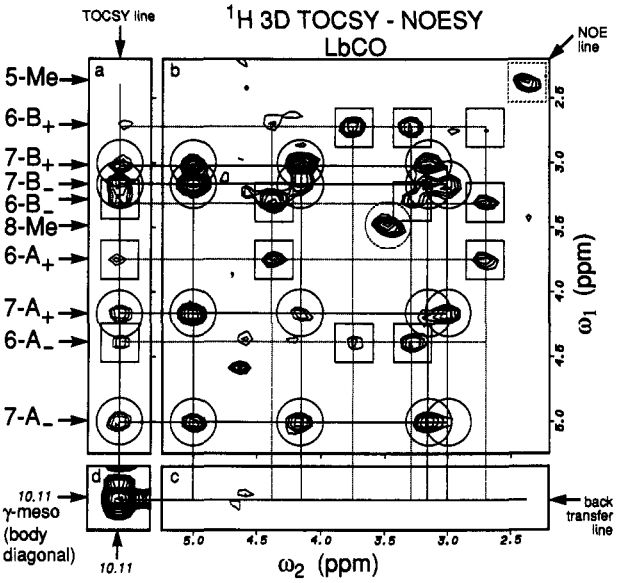

Figure 2. Plane of a homonuclear TOCSY–NOESY spectrum (with 60-ms TOCSY and 175-ms NOESY mixing times, respectively) at 10.11 ppm corresponding to the γ-meso heme proton of LbCO (pH 7). Cross-peaks involving 7- and 6-propionate protons are indicated by solid circles and squares, respectively. The labeling refers to protons $H_{A\pm}$ and $H_{B\pm}$ (see text). NOE transfers are observed between the γ-meso (body diagonal peak of the 3D cube in panel d) and the propionate protons along the diagonal (NOE line in panel b). NOEs involving the 8- and 5-methyls are indicated by dotted circles and dotted squares in panel b. Off-diagonal cross-peaks due to TOCSY transfer correspond to the propionate spin systems. ROE cross-peaks with negative sign are observed between the γ-meso and the propionate protons along the TOCSY line which does not contain pure TOCSY cross-peaks (indicated by dotted contour lines in panel a). In panels a and c, both positive and negative levels are plotted, and in panels b and d, only positive levels are plotted. The spectrum was collected at 308 K on a 600-MHz NMR spectrometer.

3D NMR spectra. The 3D cross-peaks give information on relayed magnetization transfer where all three protons are involved, and in most cases the spin systems associated with them can be uniquely defined via scalar J coupling or cross-relaxation transfer.

In the present work, the difficulty for assigning the propionate resonances using 2D methods alone has been overcome using 3D spectra, at the expense of longer data collection times; however, single-scan homonuclear 3D pulse sequences have been suggested[8h] which promise to reduce the spectral acquisition time to about 1 day.

Homonuclear 3D TOCSY–NOESY and NOESY–NOESY spectra of the diamagnetic carbon monoxide complex of soybean LbCO are used in the present work. The method used for spin system identification consists of three consecutive steps: (a) identification of NOEs from the previously assigned γ-meso proton[11,17a,b] to both 6-propionate and 7-propionate protons, (b) assignment of the two spin systems corresponding to the two propionates using TOCSY correlations, and (c) identification of NOEs from the previously assigned 5- and 8-methyls[11,17a,b] in order to distinguish the 6-propionate from the 7-propionate, respectively. The previously assigned heme resonances are confirmed using the 3D spectra in a straightforward way.

Figure 2 shows the TOCSY–NOESY (ω_1,ω_2) plane at ω_3 = 10.11 ppm[21] corresponding to the heme γ-meso proton frequency. The plane diagonal ($\omega_1 = \omega_2$, NOE line) corresponds to NOE transfers involving the spin resonating at the body diagonal frequency (here the γ-meso spin) with several other spins, some of which are additionally correlated along the ω_1 and ω_2 axes via TOCSY transfers to other spins of the same spin system. NOEs involving the eight propionate protons and the 5- and 8-methyls

(13) Hare Research Inc., Bothell, WA.
(14) Bernstein, F. C.; Koetzle, T. F.; William, G. J. B.; Meyer, E. F., Jr.; Brice, M. D.; Rodgers, J. R.; Kennard, O.; Shimanouchi, T.; Tasumi, M. *J. Mol. Biol.* **1977**, *112*, 535–542.
(15) Tripos Associates, St. Louis, MO.
(16) Brooks, B. R.; Bruccoleri, R. E.; Olafsen, B. D.; States, D. J.; Swaminathan, S.; Karplus, M. *J. Comput. Chem.* **1983**, *4*, 187–217.
(17) (a) Mabbutt, B. C.; Wright, P. E. *Biochim. Biophys. Acta* **1983**, *744*, 281–290. (b) Narula, S. S.; Dalvit, C.; Appleby, C. A.; Wright, P. E. *Eur. J. Biochem.* **1988**, *178*, 419–435. (c) Mabbutt, B. C.; Wright, P. E. *Biochim. Biophys. Acta* **1985**, *832*, 175–185. (d) Dalvit, C.; Wright, P. E. *J. Mol. Biol.* **1987**, *194*, 329–339. (e) Cooke, R. M.; Wright, P. E. *Eur. J. Biochem.* **1987**, *166*, 409–414. (f) Keller, R. M.; Wüthrich, K. In *Biological Magnetic Resonance*; Berliner, L. J., Reuben, J., Eds.; Plenum Press: New York, 1981; Vol. 3, pp 1–52.
(18) (a) Lecomte, J. T. J.; Cocco, M. J. *Biochemistry* **1990**, *29*, 11057–11067. (b) Chau, M.-H.; Cai, M. L.; Timkovitch, R. *Biochemistry* **1990**, *29*, 5076–5087. (c) Detlefsen, D. J.; Thanabal, V.; Pecoraro, V. L.; Wagner, G. *Biochemistry* **1990**, *29*, 9377–9386. (d) Santos, H.; Turner, D. L. *FEBS Lett.* **1987**, *226*, 179–185. (e) Feng, Y.; Roder, H.; Englander, S. W. *Biophys. J.* **1990**, *57*, 15–22.
(19) (a) Janson, T. R.; Katz, J. J. *J. Magn. Reson.* **1972**, *6*, 209–220. (b) Deeb, R. S.; Peyton, D. H. *Biochemistry* **1992**, *31*, 468–474.
(20) Clore, G. M.; Gronenborn, A. M. *Annu. Rev. Biophys. Biophys. Chem.* **1991**, *20*, 29–63.

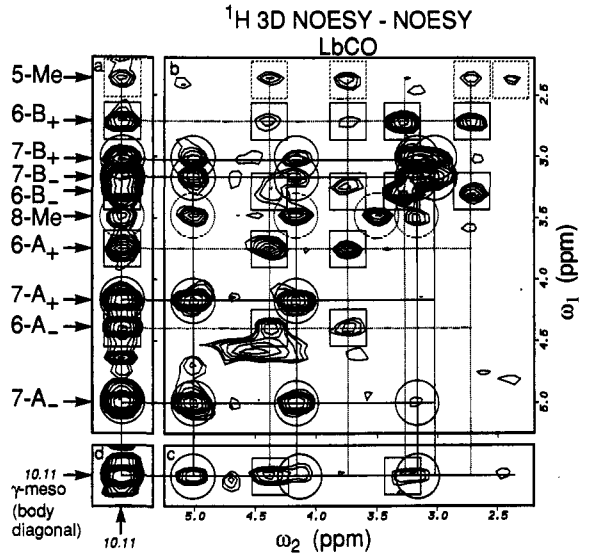

Figure 3. Same cross sections as in Figure 2 but from the NOESY–NOESY ^{1}H 3D spectrum (100-ms mixing time for both mixing periods) of LbCO (pH 7). Cross-peak labeling and notation is as in Figure 2. All 3D cross-peaks involve NOE transfer to the γ-meso proton (panel d). Cross-peaks involving the 8- and 5-methyls are shown in dotted circles and dotted squares, respectively. NOEs between the 8-methyl and the 7-propionate and between the 5-methyl and the 6-propionate protons correlate well with intra-residue NOEs within the propionate spin systems (off-diagonal cross-peaks in dotted circles and dotted squares, respectively, panel b). Cross-peaks along the NOE lines with $\omega_1 = \omega_2$ (diagonal line, panel b) and $\omega_2 = \omega_3$ (panel a) and the back-transfer NOE line with $\omega_1 = \omega_3$ (panel c) involve magnetization transfer between only two protons. The spectrum was collected at 308 K on a 600-MHz NMR spectrometer.

(at 2.41 and 3.51 ppm, respectively, in ω_3[21]) are marked in the figure. Intra-propionate proton correlations are manifested as off-diagonal 3D peaks connecting diagonal 2D-type NOE peaks. Rotating-frame NOE transfers (ROE)[22] are seen along the TOCSY line ($\omega_2 = \omega_3$), which is otherwise empty due to the absence of resolved J couplings to the γ-meso proton. As expected, the ROEs are in agreement with the corresponding NOE transfers along the diagonal. The appearance of ROE transfers, which occur with a positive rate (negative cross-peaks if diagonal peaks are positive), are normally undesirable features in 2D TOCSY spectra since they attenuate the intensity of the corresponding TOCSY peaks.[23] However, in the present context they provide additional information for identifying all propionate resonances. No cross-peaks are found on the back-transfer line ($\omega_1 = \omega_3$), which would reflect two-step ROE–NOE transfers starting and ending on the γ-meso proton, due to their intrinsically low sensitivity as a consequence of their r^{-12} internuclear distance dependence. ROE cross-peaks between the propionate and the γ-meso protons are also present in 2D TOCSY spectra, and as in the 3D TOCSY–NOESY case, they can play a key role for assignments.

Figure 3 shows the NOESY–NOESY (ω_1,ω_2) plane at ω_3 = 10.11 ppm corresponding again to the frequency of the heme γ-meso proton. 2D-type cross-peaks along the NOE (cross-diagonal) lines with $\omega_1 = \omega_2$, $\omega_2 = \omega_3$, and $\omega_1 = \omega_3$, involving NOEs between two spins, and 3D cross-peaks with $\omega_1 \neq \omega_2 \neq \omega_3$, involving double magnetization transfer between three spins, form distinct peak patterns for the two propionate spin systems. Furthermore, NOEs are observed between the γ-meso and the 5- and 8-methyl protons, which also exhibit true 3D cross-peak networks with the 6- and 7-propionate protons, respectively. The lower intensity of the cross-peaks along the back-transfer NOE line ($\omega_1 = \omega_3$) compared to NOE lines with $\omega_1 = \omega_2$ and $\omega_2 = \omega_3$ reflects the difference between the r^{-12} and r^{-6} internuclear distance dependences, respectively.

On the basis of the cross-peak intensities, the geminal proton pairs, which are in the following called A and B pairs, can be readily found, and the four propionate protons for each of the two propionates are labeled according to the position of their resonances on the chemical shift axis H_{A-}, H_{A+}, H_{B-}, and H_{B+}, where A_ is the downfield resonance and A_+ the upfield resonance of proton pair A; the labeling of the resonances of pair B is analogous.

The propionate spin system assignment procedure described here relies on the assignments of the γ-meso and 5- and 8-methyl protons. In the case of LbCO, these assignments are available.[11,17a,b] However, in the absence of these, assignment methods for all heme meso and methyl protons and the protons of the asymmetrically placed vinyl groups have been previously described, most of which are based on a unique intra-heme NOE connectivity pattern.[11,17-19] From assignments of meso protons which resonate in a characteristic downfield region (9–10.5 ppm) due to the influence of the large heme ring current effect, NOEs to other heme protons can be identified. In addition, TOCSY and double-quantum spectra are important for completion of the vinyl proton assignments.

In summary, homonuclear 3D spectra have proved to be very useful for the identification of all heme protons and the pairing of geminal propionate protons. Used on a qualitative basis, however, they do not allow assignment of the geminal proton pairs to the α- or β-carbon positions. In order to achieve this and to gain information about the stereospecific assignments and conformations, more quantitative information is required as discussed in the next section. The method proposed here for propionate spin system assignments can be readily applied to other diamagnetic complexes of heme proteins.

4. Proton Assignments and Conformations of Heme Propionates

The required structural data are provided by 2D NOESY and 2QF-COSY experiments in the form of inter-proton distance and torsion angle information. The next step aims at using the information obtained from the 3D spectra to identify a maximum number of cross-peaks arising from heme protons in the corresponding 2D NOESY and 2QF-COSY spectra (Figure 4). It should be emphasized at this point that unambiguous propionate spin system identification using 2D spectra alone is very difficult due to resonance overlap. Figure 4 shows the propionate proton region of a 2QF-COSY spectrum, where intra-residue cross-peaks of the 6- and 7-propionates are indicated by solid squares and circles, respectively. As a consequence of their large J coupling constant, the geminal cross-peaks are clearly visible. More interestingly, the vicinal cross-peak intensities vary significantly within both propionates such that some of the expected COSY peaks are absent. This observation shows directly that the corresponding ^3J coupling constants are not subject to extensive conformational averaging and that the propionates are rather restricted in their mobility about χ_2. To gain further insight, the Karplus relationships[24,25] for alkane torsion angles, generalized to include substituent effects,[26] are applied to the propionate systems

(21) Chemical shifts are accurate within 0.01 ppm when measured in ω_3 and within 0.03 ppm when measured in ω_1 or ω_2 due to the inherent lower digital resolution along the ω_1 and ω_2 dimensions of the homonuclear 3D spectra.

(22) Bothner-By, A. A.; Stephens, R. L.; Lee, J.-M.; Warren, C. D.; Jeanloz, R. W. *J. Am. Chem. Soc.* **1984**, *106*, 811–813.

(23) Griesinger, C.; Otting, G.; Wüthrich, K.; Ernst, R. R. *J. Am. Chem. Soc.* **1988**, *110*, 7870–7872.

(24) Karplus, M. *J. Chem. Phys.* **1959**, *30*, 11–15.

(25) Bystrov, V. F. *Prog. Nucl. Magn. Reson. Spectrosc.* **1976**, *10*, 41–81.

(26) Haasnoot, C. A. G.; De Leeuw, F. A. A. M.; Altona, C. *Tetrahedron* **1980**, *36*, 2783–2792.

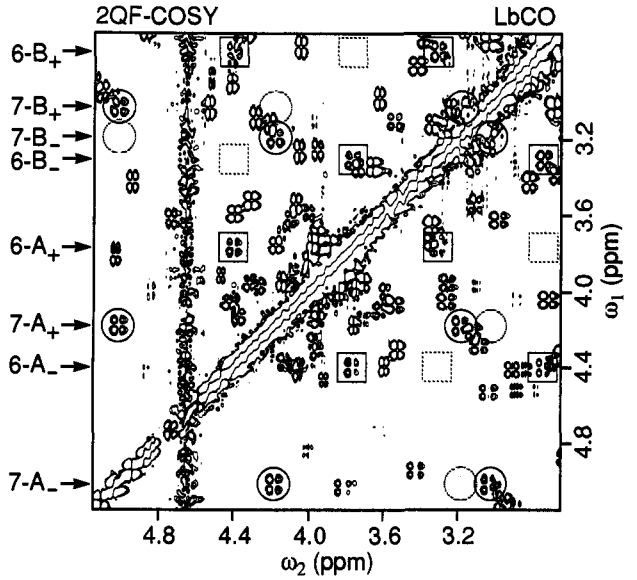

Figure 4. Section of the 2QF-COSY spectrum of LbCO (pH 7). Cross-peaks corresponding to 7-propionate and 6-propionate protons are indicated by circles and squares, respectively. The labeling refers to the $H_{A\pm}$ and $H_{B\pm}$ propionate protons (see text). Dotted circles and squares in the COSY spectrum refer to cross-peaks that are absent due to small $^3J_{A\pm,B\pm}$ coupling constants. The spectrum was collected at 308 K on a 600-MHz NMR spectrometer.

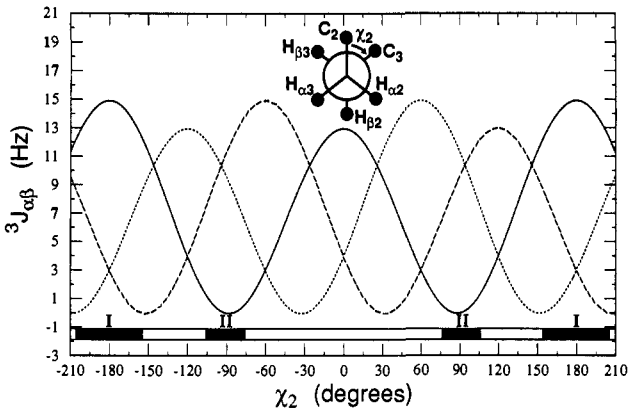

Figure 5. Plots of the generalized Karplus relations for the propionate spin systems.[26] The inset shows the notation and conformation used for a projection of the methylene groups as viewed down the $C_\alpha C_\beta$ bond (the labeling of the carbon atoms corresponds to the notation of Figure 1). The different curves correspond to the various vicinal J coupling partners: $J_{\alpha2,\beta2}$ and $J_{\alpha3,\beta3}$ (solid line), $J_{\alpha2,\beta3}$ (dotted line), and $J_{\alpha3,\beta2}$ (dashed line). The shaded regions at the bottom correspond to the χ_2 torsion angle space compatible with the cross-peak intensity pattern observed in the 2QF-COSY spectra of Figure 4. Regions I and II span the ranges $\chi_2 = 180 \pm 25°$ and $\chi_2 = \pm 90 \pm 15°$, respectively.

$$^3J_{\alpha2,\beta2}(\chi_2) = {}^3J_{\alpha3,\beta3}(\chi_2) = {}^3J_{\alpha2,\beta3}(\chi_2 - 120°) = {}^3J_{\alpha3,\beta2}(\chi_2 + 120°) \quad (1)$$

and are plotted in Figure 5. It should be noted that in the present context the inclusion of substituent effects into the Karplus relationships is of minor importance for the discussion of the intensity pattern observed in the 2QF-COSY spectrum (Figure 4). Torsion angle definition and proton labeling are given in the inset of Figure 5. The shaded areas at the bottom of Figure 5 show the intervals of the propionate χ_2 torsion angle values that are compatible with the peak intensity patterns found in the 2QF-COSY spectrum of Figure 4. An estimated line width of about 25 Hz renders a quantitative measurement of coupling constants from the 2QF-COSY peaks unrealistic. Nevertheless, using only qualitative features of the 2QF-COSY spectrum, namely the *presence* and *absence* of cross-peaks, and assuming that the

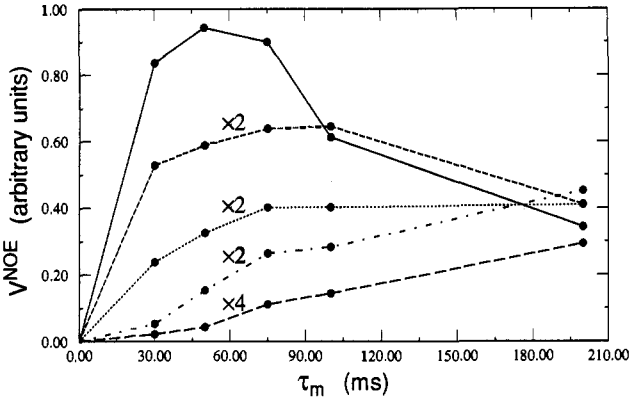

Figure 6. NOE buildup curves for selected cross-peaks from 2D NOESY spectra collected with mixing times of 30, 50, 75, 100, and 200 ms. They correspond to 7-propionate geminal A_+/A_- (solid line), vicinal B_-/A_- (dotted line), A_-/γ-meso (dashed line), 8-methyl/A_- (dotted–dashed line), and 8-methyl/γ-meso (long dashed line) cross-peaks. The curves are individually scaled as indicated.

propionate protons have comparable line widths, the Karplus curves imply that only very narrow χ_2 torsion angle ranges around $180 \pm 25°$ and $\pm 90 \pm 15°$ (regions I and II of Figure 5, respectively) are compatible with experiment. Furthermore, the observed intensity pattern of the cross-peaks imposes some restrictions on relative stereospecific assignments of the α and the β protons. For instance, for either propionate with $\chi_2 = 180°$, if H_{A-} occupies stereospecific position 2, *e.g.* $H_{\alpha2}$, then H_{B+} must also occupy the same stereospecific position 2, *i.e.* $H_{\beta2}$. On the other hand for $\chi_2 = \pm 90°$, if H_{A-} occupies stereospecific position 2, *e.g.* $H_{\alpha2}$, then H_{B+} must occupy position 3, *i.e.* $H_{\beta3}$. To exemplify this argument, the cross-peak $H_{A-}H_{B+}$ of the 2QF-COSY spectrum (Figure 4), in view of the Karplus relations (Figure 5), could be assigned either to $H_{\alpha2}H_{\beta2}$ or to $H_{\alpha3}H_{\beta3}$ for $\chi_2 = 180°$ or either to $H_{\alpha2}H_{\beta3}$ or to $H_{\alpha3}H_{\beta2}$ for $\chi_2 = \pm 90°$. Similar arguments apply to all cross-peaks present in the 2QF-COSY spectrum. This additional restriction for stereo assignments allows us to discriminate between structures that fit the NOESY data equally well, as will be shown below.

Due to the lack of a coupling partner on the heme, the 2QF-COSY spectrum provides no information regarding the χ_1 angles and information from the NOESY experiment alone has to be used. To assess the relevance of spin diffusion, which can be rather severe in large molecules,[27] NOE buildup curves for selected cross-peaks involving propionate protons have been measured. The behavior of characteristic cross-peaks for 7-propionate is plotted in Figure 6 for geminal, vicinal, propionate/γ-meso, methyl/propionate, and methyl/γ-meso proton NOE cross-peaks. Spin-diffusion effects are most evident for weak NOEs corresponding to larger internuclear distances, *e.g.* the 8-methyl/γ-meso NOE (~5.5 Å), indicating the presence of an intervening relay spin. The geminal peaks reach their maximum intensity at rather short mixing times around 50 ms, reflecting the short T_1 relaxation times which are due to the slow overall rotational tumbling dominated by the power spectral density function sampled at zero frequency.

The NOESY spectrum with $\tau_m = 30$ ms has been chosen for the quantitative extraction of peak volumes, which are analyzed using the grid search procedure described below. The procedure exploits the fact that no NOEs are observed between the two propionates and they may therefore be treated independently. For each propionate, a set of 1296 different conformations has been generated on a grid in the two rotatable torsion angles χ_1 and χ_2 with a grid size of 10° using CHARMM.[16] Relative intensities for all intra-heme NOEs have been calculated on the

(27) Wüthrich, K. *NMR of proteins and nucleic acids*; Wiley-Interscience: New York, 1986.

basis of the r^{-6} distance dependence of cross-relaxation rates in a rigid isotropically tumbling molecule, assuming that the propionates are adequately described by a static single-structure model. An exception is made for NOEs to the methyl groups where the two limiting cases of slow and fast rotation of the methyl protons about the symmetry axis have been taken into account. In the slow-motion regime ($\tau_{int} \gg \tau_c$, where τ_{int} is the methyl group rotation correlation time and τ_c is the overall tumbling correlation time), the cross-relaxation rate Γ_{ik}^{NOE} between proton i and methyl group k is given by[28]

$$\Gamma_{ik}^{NOE} \propto \sum_{\mu=1}^{3} r_{ik,\mu}^{-6} \qquad (2)$$

Correspondingly, for fast internal rotation ($\tau_{int} \ll \tau_c$)

$$\Gamma_{ik}^{NOE} \propto \frac{1}{3}\sum_{\mu,\nu=1}^{3} \frac{P_2(\cos\theta_{\mu\nu}^{ik})}{r_{ik,\mu}^{3} r_{ik,\nu}^{3}} \qquad (3)$$

where $\theta_{\mu\nu}^{ik}$ is the angle between the two vectors with lengths $r_{ik,\mu}$ and $r_{ik,\nu}$ from spin i to methyl proton sites μ and ν, respectively. $P_2(x) = (3x^2 - 1)/2$ is the second-order Legendre polynomial. Averaged methyl group coordinates have been taken from the neutron structure of MbCO.[4c]

For the evaluation of the conformation which fits best the measured NOE cross-peak volumes, a weighted-root-mean-square deviation Q for predicted and experimental volumes has been calculated for each grid structure

$$Q = \{\sum_i (V_i^{exp} + V_0)^{-1/2}(V_i^{exp} - \kappa V_i^{theor})^2\}^{1/2} \qquad (4)$$

where κ represents a relative scaling factor which is determined in a least-squares sense by minimizing Q. The volume V_0 has been set to 8% of the largest cross-peak and prevents overemphasis of the less accurately defined weak cross-peaks. Calibration based on the knowledge of the internuclear distance of geminal proton pairs was not used due to their deviation from linearity even for short mixing times, as shown in the buildup curves of Figure 6; such a calibration would lead to a systematic underestimation of larger distances.

For any given grid structure, Q has been evaluated for all possible alternative assignments including both changes in stereo assignments and swapping between the α- and the β-carbon positions. In this regard, the method deviates from other procedures where assignment is done prior to structure determination;[9,10] here, the two goals are combined in a single step. To restrict the search, all geminal proton pairs, which have been established on the basis of the 3D (and confirmed by the 2D) spectra, are not separated. This leads to a total of eight different possible assignments. Although the methyl protons do not perfectly reflect mirror symmetry with respect to the heme plane, it is clear that otherwise the available intra-heme NMR data do not allow the two symmetric solutions to be distinguished. Hence, a structure with torsion angles χ_1 and χ_2 and a given assignment yields almost the same value of Q as the structure with $-\chi_1$ and $-\chi_2$ and reversed stereo assignments. Consequently, because of the plane of symmetry, only four different assignments are relevant.

The torsion angles of the best-fitting structures for the four assignments are given together with their penalty function values Q in Table I. In the course of the grid search, Q can take values between 8.4 and 43.8. For assignment 1, H_{A-} corresponds to $H_{\alpha 2}$, H_{A+} to $H_{\alpha 3}$, H_{B-} to $H_{\beta 2}$, and H_{B+} to $H_{\beta 3}$, respectively; assignment 2 corresponds to assignment 1 but with interchanged stereospecific assignments for H_{A-} and H_{A+}; assignment 3 corresponds to assignment 1 but with interchanged assignments for the H_A and H_B protons; assignment 4 corresponds to assignment 2 but with interchanged assignments for the H_A and H_B protons. For the 6- and 7-propionates, the best-fitting structures require assignment 2 and have torsion angles $\chi_1 \approx 90°$ and $\chi_2 \approx 170°$ or $\chi_2 \approx 160°$, respectively. Table I gives the penalty function for the different assignments together with the scalar ^3J coupling constants calculated for all four structures using eq 1. The structures yielding the lowest Q values also explain the observed COSY cross-peaks. Hence, the NOESY and COSY data are consistent.

Table I. Best-Fitting Conformations and Assignments with Respect to the NOESY Peak Intensities[a]

	assignment[b]			
	1	2	3	4
	6-Propionate[c]			
χ_1/χ_2	−80°/−60°	90°/170°	−50°/−100°	−60°/−160°
Q[d]	10.1	8.4	20.5	18.0
$^3J_{\alpha 2,\beta 2}$, $^3J_{\alpha 2,\beta 3}$	3.1, 2.9	14.5, 1.3	0.5, 11.3	13.2, 7.5
$^3J_{\alpha 3,\beta 2}$, $^3J_{\alpha 3,\beta 3}$	14.9, 3.1	5.0, 14.5	9.0, 0.5	0.2, 13.2
	7-Propionate[e]			
χ_1/χ_2	180°/−50°	90°/160°	40°/−90°	−10°/−140°
Q	11.5	10.2	14.9	14.0
$^3J_{\alpha 2,\beta 2}$, $^3J_{\alpha 2,\beta 3}$	5.2, 1.2	13.3, 0.3	0.0, 9.5	8.8, 11.4
$^3J_{\alpha 3,\beta 2}$, $^3J_{\alpha 3,\beta 3}$	14.4, 5.2	7.3, 13.3	11.4, 0.0	0.6, 8.8

[a] NOESY mixing time of 30 ms. [b] See text for definition of assignments. [c] Best results for fast methyl group rotation. [d] Penalty function described in text. [e] Best results for slow methyl group rotation.

Table II. Experimental and Back-Calculated Relative NOESY Peak Volumes for the Best Grid Structures

	6-propionate (χ_1/χ_2: 90°/170°)		7-propionate (χ_1/χ_2: 90°/160°)	
proton pair	exptl[a]	model[b]	exptl[a]	model[b]
H_γ–Me[c]	1.3	1.0	1.6	1.0
H_γ–$H_{\alpha 3}$	65.9	79.0	79.3	68.1
H_γ–$H_{\alpha 2}$	14.8	3.7[d]	25.1	3.3[d]
H_γ–$H_{\beta 2}$	29.9	31.9	26.6	28.9
H_γ–$H_{\beta 3}$	6.7	2.9	7.9	3.1
H_β/H_δ–Me[e]	86.5	70.9	105.0	107.3
Me–$H_{\alpha 3}$	2.3	4.6	7.9	4.9
Me–$H_{\alpha 2}$	56.7	52.7	(43.2)[f]	76.6
Me–$H_{\beta 2}$		2.2	(28.7)	2.1
Me–$H_{\beta 3}$		18.2	19.7	20.3
$H_{\alpha 2}$–$H_{\alpha 3}$	[217.0][f]	328.6	[251.0]	284.2
$H_{\alpha 3}$–$H_{\beta 2}$	47.6	48.5	35.7	45.3
$H_{\alpha 3}$–$H_{\beta 3}$		12.1	9.6	10.4
$H_{\alpha 2}$–$H_{\beta 2}$		12.2	(22.9)	10.6
$H_{\alpha 2}$–$H_{\beta 3}$	31.9	34.3	25.7	25.5
$H_{\beta 2}$–$H_{\beta 3}$	[197.0]	304.5	[101.0]	256.3

[a] Experimental NOESY cross-peak volumes (in arbitrary units) extracted from a 30-ms NOESY spectrum and located above the diagonal. [b] Back-calculated peaks from best-fitting grid structures; no spin-diffusion effects included. [c] Refers to 5-methyl for 6-propionate or 8-methyl for 7-propionate. [d] Inclusion of intra-heme spin diffusion in the NOE back-calculation slightly improves the agreement between the observed and calculated values for this NOE (see text); however, spin diffusion including external protein protons has not been attempted. [e] Refers to NOEs involving H_β (β-meso) with 5-methyl and H_δ (δ-meso) with 8-methyl, respectively. [f] Volumes in enclosures have not been used in the fit. Parentheses denote ambiguity in the integration due to overlap and/or presence of t_1 noise. Brackets indicate NOE volumes of the geminal proton pairs which suffer from significant T_1 relaxation even at 30-ms mixing time (see text).

The back-calculated NOESY cross-peak volumes are listed in Table II together with the experimental volumes. The values in brackets have not been included in the fits since the peak integration was affected by distortions or by overlaps with neighboring cross-peaks. The largest violation is found for both propionates for the peaks between H_γ and $H_{\alpha 2}$, which is larger in the experiment than predicted by the model. Inclusion of spin diffusion in the back-calculation yields a better agreement in this case, since the intervening spin of $H_{\alpha 3}$ can relay the magnetization between H_γ and $H_{\alpha 2}$. Overall, however, the inclusion of spin

(28) Tropp, J. *J. Chem. Phys.* **1980**, *72*, 6035–6043.

diffusion in the back-calculations does not give lower penalty values, which indicates a non-negligible role of surrounding protein protons. In addition, the remaining discrepancy between experimental and the modeled data is due to the finite grid size of 10° and local structural fluctuations. The presence of a low population of a second conformation cannot be excluded with certainty on the basis of the present data.

As mentioned above, the exclusive use of intra-heme proton information cannot discriminate between $\chi_1 = +90°$ or $\chi_1 = -90°$ due to the symmetry introduced by the heme plane. In order to resolve this ambiguity, external NOEs between propionate protons and assigned resonances of proximal and distal heme pocket residues[11,17a,b] were identified. For 6-propionate, the observed NOEs between the β protons and the δ and ϵ protons of the distal residues at the CD corner, Phe44 and Phe46, are consistent with $\chi_1 = +90°$; *i.e.*, the 6-propionate chain extends into the distal side of the heme pocket. The corresponding interproton distances in the X-ray structures of the acetate and cyanide complexes of lupin Lb (residues Phe44 and Phe46 are conserved in soybean and lupin Lbs) are consistent with the NOE data. The presence of NOEs between the most upfield-shift methyl resonance of the proximal side residue Val91 and the α protons of 6-propionate and the absence of NOEs between this methyl and the propionate β protons are also consistent with $\chi_1 = +90°$. In this conformation, the α-carbon is in the plane of the heme and the α protons protrude toward the proximal heme pocket side while the β protons clearly extend into the distal side of the heme pocket. The 6-propionate conformation in soybean LbCO ($\chi_1 \approx +90°$, $\chi_2 \approx 170°$) is thus similar to that of the published crystal structures of lupin leghemoglobins.

For the 7-propionate, NOEs are observed between the β-methylene protons and the methyls of Val91 and Leu88 in the F-helix, on the proximal side of the heme pocket. The corresponding interproton distances in the X-ray structure of the cyanide complex of lupin leghemoglobin (soybean Lb residues Leu88 and Val91 are homologous to lupin Lb residues Leu93 and Val96, respectively) are in agreement with the NOE data. The presence of additional medium-intensity NOEs between the δ proton of the distal histidine, His61 (E7), and the α protons of 7-propionate and the absence of NOEs (at $\tau_m \leq 50$ ms) to the β protons of 7-propionate confirm a conformation with $\chi_1 \approx +90°$. In this orientation, the α protons lie slightly above the heme plane toward the distal side and the β protons project into the proximal heme pocket. NOEs between the δ proton of His61 and the heme γ-meso and 8-methyl protons indicate proximity of the His61 $C_\delta H$ to the heme plane. Both the observed NOEs and ring current shifts indicate conformational differences for the distal histidine between LbCO in solution and the X-ray structure of lupin LbCN.[17b] The 7-propionate conformation ($\chi_1 \approx +90°$, $\chi_2 \approx 160°$) is thus similar to that in the crystal structure of lupin LbCN and is the mirror image of that reported for a number of lupin Lb structures, including the acetate, aquomet, deoxy, fluoride, nicotinate, and nitrobenzene complexes.[4f-h] The similarity of the 7-propionate conformations in the CO and CN^- complexes of soybean and lupin Lbs, respectively, is not surprising, given that both CO and CN^- prefer a linear end-on coordination geometry.

The availability of stereospecific propionate assignments eliminates the need for pseudoatom correction in distance geometry calculations and greatly increases the precision with which local structures can be calculated from NOE data. Also, propionate assignments aid in identification of additional NOEs to heme pocket protons, thus increasing the number of available distance constraints for structure calculation. This can be valuable in calculating well-defined NMR heme pocket structures and in assessing the role of propionate hydrogen bonds and salt bridges with nearby residues in anchoring the heme in a unique configuration within the heme pocket.[1a,b]

Table III. ^1H NMR Chemical Shifts and Assignments for the Heme Propionates[a]

	6-propionate		7-propionate	
soybean LbCO[b]	$H_{\alpha 2}$, $H_{\alpha 3}$ 3.78, 4.41	$H_{\beta 2}$, $H_{\beta 3}$ 3.31, 2.74	$H_{\alpha 2}$, $H_{\alpha 3}$ 4.19, 5.02	$H_{\beta 2}$, $H_{\beta 3}$ 3.19, 3.04
	H_α, $H_{\alpha'}$	H_β, $H_{\beta'}$	H_α, $H_{\alpha'}$	H_β, $H_{\beta'}$
desFe SW Mb[c]	4.31, 3.71	2.86, 2.66	3.34, 3.06	5.02, 4.30
desFe horse Mb[c]	4.34, 3.71	2.79, 2.59	3.35, 3.07	5.02, 4.33
cytochrome c_{551}[d]	4.57, 4.26	3.43, 2.67	4.68, 3.90	3.35, 2.72
cytochrome c_{551}[e]	4.57, 4.22	3.41, 2.63	4.62, 3.88	3.34, 2.69
cytochrome c'[f]			4.16, 3.61	
cytochrome c^8[g]	4.19		4.17, 3.64	
PP IX dimethyl ester[h]	4.27, 4.27	3.16, 3.16	4.27, 4.27	3.16, 3.16
SnPP[i]	4.59, 4.59	3.25, 3.25	4.59, 4.59	3.25, 3.25
$(SnPP)_2$[j]	4.63, 4.52	3.16, 3.05	4.63, 4.52	3.16, 3.05

[a] All chemical shifts in ppm; samples in aqueous buffers unless otherwise noted. [b] pH 7, 308 K; chemical shifts reported here are measured in the ω_3 dimension of the 3D spectra and they are within ≤0.01 ppm from those measured in the higher digital resolution 2D NOESY spectra. The corresponding stereospecific assignments are for $\chi_1 = +90°$ for both propionates, which is distinguished from the alternative $\chi_1 = -90°$ value on the basis of NOEs observed between the propionate protons and side chain protons of heme pocket residues (see text). [c] From ref 18a; pD 5.7, 298 K, SW = sperm whale. [d] From ref 18b; pH 3.5, 333 K. [e] From ref 18c; pH 6.8, 298 K. [f] From ref 18d; pH 6.8, 303 K. [g] From ref 18e; pH 5.7, 293 K. [h] From ref 19a; in $CDCl_3$, 294 K. [i] From ref 19b; pH 11.5, 298 K. [j] From ref 19b; pH 7.5, 298 K.

In summary, the methodology presented is suitable to determine the conformation of a ligand bound to a larger protein and could be used to study local structural features of the protein itself. Application and extensions of the method for studying nucleic acid fragments[29] and selectively labeled cofactors or parts of large proteins are conceivable using heteronuclear editing techniques.[30]

5. Comparison with Other NMR and X-ray Studies

Table III summarizes the published propionate proton assignments for free protoporphyrin IX,[19] desFe Mb[18a] (no Fe atom present), and cytochromes c and c_{551}[18b-e] and compares them with the proton assignments for soybean LbCO. The degeneracy of the propionate α- and β-proton resonances observed in free porphyrins is always removed in the presence of the protein. In most of the earlier studies it was not possible to discriminate between the α and β protons by using NOE intensities alone or by comparison to crystal structures. However, assignments were made by comparison of the chemical shift values with those of free porphyrins[19] (Table III). Assignments based on chemical shifts are expected to be reliable in the present case since the heme ring current contribution has a dominant effect. The propionate assignments reported in the literature are in good agreement with ours, with the exception of those for desFe Mb,[18a] where the α and β resonances of the 7-propionate are reversed (see Table III). This is the first time complete stereospecific assignments for heme propionate protons have been made.

Different conformations have been observed for the propionate groups of various heme proteins. A representative selection of propionate structures of heme-protein crystal structures deposited in the Brookhaven Protein Data Bank is given in Table IV.[31] We note a discrepancy for the 7-propionate χ_2 torsion angle in the X-ray and the neutron diffraction structures of MbCO.[4b,c] With the exception of χ_2 for 7-propionate in the neutron diffraction study,[4c] all χ_2 torsion angles are characteristic for staggered conformations of the propionate β-methylene groups.

Our analysis for soybean LbCO indicates $\chi_1 \approx 90°$ for both propionates and $\chi_2 \approx 170°$ and 160° for 6-propionate and 7-propionate, respectively (see Table I). These angles are similar

(29) Ellman, J. A.; Volkman, B. F.; Mendel, D.; Schultz, P. G.; Wemmer, D. E. *J. Am. Chem. Soc.* **1992**, *114*, 7959–7961.
(30) (a) Wörgötter, E.; Wagner, G.; Wüthrich, K. *J. Am. Chem. Soc.* **1986**, *108*, 6162–6167. (b) Senn, H.; Otting, G.; Wüthrich, K. *J. Am. Chem. Soc.* **1987**, *109*, 1090–1092.

Table IV. Torsion Angles of Heme Propionates for Selected Heme Proteins

protein	PDB file	6-propionate χ_1[c]	6-propionate χ_2[c]	6-propionate H-bond[a]	7-propionate χ_1	7-propionate χ_2	7-propionate H-bond[b]
soybean Lb							
LbCO[d]		90.0	170.0		90.0	160.0	
lupin Lb							
metLb acetate[4f]	2lh1	89.9	165.5	p(Ser45)	−110.4	−175.0	a
LbCN[4h]	2lh3	81.0	163.9	p(Ser45)	100.1	175.0	a
sperm whale Mb							
metMb[4a]	4mbn	96.5	177.7	p(Arg45)	102.2	−54.2	p(His97)
MbCO(X-ray)[4b]	1mbc	72.9	166.5	p(Arg45)	104.4	−54.0	p(His97)
MbCO(neutron)[4c]	2mb5	91.9	179.0	p(Arg45)	76.0	9.0	p(His97,Ser92)
MbO_2[4j]	1mbo	91.3	176.6	p(Arg45)	104.3	−58.3	p(His97)
A. limacina Mb							
metMb[4e]	1mba	53.4	102.6	a	−92.7	−175.4	a
G. dibranchiata Hb[e]							
HbCO[4n]	1hbg	76.2	64.3	p(Arg89)	126.6	155.7	a
erythrocruorin[e]							
HbCO[4o]	1eco	98.1	−68.8	p(Arg90)	84.8	−175.8	p(His58)
human Hb							
deoxyHb[4p]	4hhb						
(heme α)		71.8	172.8	p(His45)	92.4	156.5	a
		88.9	−169.7	p(His45)	83.9	177.1	a
(heme β)		82.0	−158.3	a	73.2	−165.9	a
		53.0	−160.1	a	90.0	178.7	p(Lys66)
tuna cytochrome *c*							
reduced (Fe^{2+})[4s]	5cyt	−74.9	−166.4	p[f]	−89.9	−173.5	p[f]

[a] Hydrogen bond between 6-propionate and a side chain residue; p denotes present with the donor indicated in parentheses and a denotes absent, as discussed in the appropriate references or evaluated from the PDB files. [b] Hydrogen bond between 7-propionate and a side chain residue. [c] All torsion angles in degrees, extracted from the Brookhaven Protein Data Bank files[14] using the program SYBYL.[15] [d] NMR analysis, present work. [e] The X-ray structures of *G. dibranchiata* Hb and erythrocruorin (*C. thummi thummi* Hb) demonstrate the presence of a major heme isomer which is related, by a 180° rotation about the α–γ-meso axis, to the observed "normal" orientation of the heme in sperm whale Mb and human Hb. [f] The propionates of reduced cytochrome *c* exhibit multiple hydrogen bonding, *e.g.*, 6-propionate with Thr49 and Thr78 and 7-propionate with Arg38, Tyr48, and Trp59.

to those of lupin LbCN rather than other lupin leghemoglobins, probably reflecting a ligand effect on the propionate conformations. Torsion angles of $\chi_1 \approx +90°$ and $\chi_2 \approx 180°$ for 6-propionate are common to both sperm whale myoglobin and lupin leghemoglobin complexes, as shown in Table IV. However, for 7-propionate χ_1 deviates significantly from +90° for all leghemoglobin complexes except LbCN and χ_2 deviates from 180° for all sperm whale myoglobin complexes.

The similarity of the propionate conformations of soybean LbCO (determined by NMR) and those of lupin LbCN (Table IV) suggests common hydrogen-bonding interactions between 6-propionate and a globin side chain, most likely the conserved serine 45,[4f-h] and no hydrogen bond between 7-propionate and a globin side chain. We cannot, however, exclude hydrogen bonding to solvent molecules, as observed in the X-ray structures of lupin Lb.[4f-h]

Propionate χ_1 and χ_2 torsion angles are listed in Table IV for a series of myoglobins and hemoglobins, along with observed hydrogen-bonding interactions. Inspection of the entries in Table IV for lupin Lb, sperm whale Mb, and *A. limacina* Mb reveals a strong correlation between torsion angles $\chi_1 = 87 \pm 8°$ and $\chi_2 = 169 \pm 6°$ (average and standard deviation for 13 sperm whale Mb and lupin Lb X-ray structures; see ref 31 for PDB files) and the presence of a hydrogen bond involving the 6-propionate and a globin side chain at the CD loop. The CD loop residues are Arg45 and Lys45 for sperm whale and horse myoglobins, respectively, and Ser45 for lupin leghemoglobin. *A. limacina* Mb lacks a hydrogen bond, as reflected in the propionate torsion angles, $\chi_1 \approx 60°$ and $\chi_2 \approx 90°$ (see Table IV). The situation is more complex for the 7-propionate, where a hydrogen bond between 7-propionate and a globin side chain at the FG corner (His97 for sperm whale myoglobin) corresponds to $\chi_1 = 106 \pm 10°$ and $\chi_2 = -57 \pm 4°$ (six sperm whale Mb X-ray structures are used; see ref 31 for PDB files). In proteins which lack this hydrogen bond, *A. limacina* Mbs and soybean and lupin Lbs, very different χ_1 and χ_2 dihedral angles are observed (see Table IV). The neutron diffraction study of MbCO[4c] proposes hydrogen bonding of 7-propionate not only to histidine 97 but also to serine 92 (F7), reflecting the unusual χ_2 torsion angle of this propionate side chain compared to those determined by the X-ray studies[4a,b,j-m] (Table IV).

In the case of *Glycera dibranchiata* Hb and erythrocruorin (*Chironomous thummi thummi* Hb), an equilibrium between major and minor heme isomers has been previously observed by NMR.[32] The major isomer is related by a 180° rotation about the α–γ-meso axis to the observed "normal" orientation of the heme in sperm whale Mb and human Hb. In this "reverse" isomer, the 6-propionate occupies the 7-propionate crystallographic position of the "normal" orientation and vice versa. The X-ray studies of these two proteins[4n,o] are in agreement with the presence of this isomer, explaining the observed reverse hydrogen-bonding pattern for the 6- and 7-propionates (Table IV).

The hydrogen bond–torsion angle correlation proposed above seems to be valid for the homologous monomeric hemoglobins and myoglobins which contain the "normal" heme insertion isomer and does not necessarily apply to tetrameric hemoglobins and other heme proteins. For example, in the case of human hemoglobin[4p-r] the observed hydrogen-bonding pattern is not consistent with the correlation observed in leghemoglobin and sperm whale myoglobin (Table IV). Also, in the case of cytochrome *c*[4s,t] (Table IV) ($\chi_1 \approx -90°$ and both χ_2 torsion angles

(31) The following PDB files for 28 structures have been used in the current analysis: 2lh 1–7 for the acetate, aquomet, cyanide, deoxy, fluoride, nicotinate, and nitrosobenzene complexes of lupin leghemoglobin;[4f-h] 4mbn, 5mbn, 1mbc, 1mbo, 1mbi, and 1mbw for the aquomet,[4a] deoxy,[4k] carbonmonoxy,[4b] oxy,[4j] imidazole,[4l] and aquomet recombinant Asp122[4m] complexes of sperm whale myoglobin, respectively; 2mb5 for the neutron diffraction structure of carbonmonoxy sperm whale Mb;[4c] 1mba, 4mba, and 2mba for the aquomet, imidazole, and azide complexes of *A. limacina* myoglobin, respectively;[4e] 1hbg and 2hbg for the carbonmonoxy and deoxy complexes of *G. dibranchiata* Hb, respectively;[4n] 1eco, 1eca, 1ecd, and 1ecn for the carbonmonoxy, aquomet, deoxy, and cyanide complexes of erythrocruorin, respectively;[4o] 4hhb, 2hco, and 1hho for the deoxy,[4p] carbonmonoxy,[4q] and oxy[4r] complexes of human hemoglobin, respectively; 5cyt and 3cyt for the ferrous[4s] and ferric[4t] complexes of tuna cytochrome *c*, respectively.

(32) (a) Cooke, R. M.; Wright, P. E. *Biochim. Biophys. Acta* **1985**, *832*, 365–372. (b) LaMar, G. N.; Smith, K. M.; Gersonde, K.; Sick, H.; Overkamp, M. *J. Biol. Chem.* **1980**, *255*, 66–70.

are about 180°) both propionate conformations form hydrogen bonds to neighboring protein residues (Table IV).

6. Conclusions

Homonuclear 3D TOCSY–NOESY and NOESY–NOESY spectroscopy combined with quantitative information from 2D spectra and interpreted using a novel grid search strategy represents a powerful method for assignment and structural characterization of heme propionates in heme proteins. The establishment of an additional number of NOE distance constraints between propionate protons and the heme pocket is expected to be important for the generation of high-resolution NMR structures of the environment of the binding sites in globins, which in turn are likely to provide new insights into ligand entry and exit paths and structure–function relationships.[33] Homonuclear 3D NMR appears to be generally applicable to overcome assignment problems in highly crowded spectra for proteins of moderately large molecular mass (≤16–18 kDa). The grid search technique in torsion angle space, with assignments relying on the back-calculation and comparison of NOESY cross-peak volumes and J coupling constants with experimental data, is in the case presented here able to discriminate between different solutions and allows, together with a limited number of qualitative external NOEs to the heme pocket, the identification of a unique conformation. The propionate torsion angles of LbCO determined from the NMR data, $\chi_1 \approx 90°$ and $\chi_2 \approx 180°$, correlate well with X-ray studies of a series of homologous proteins. Comparison with the X-ray structure of lupin Lb suggests that these torsion angle values might be indicative of the presence of a hydrogen bond between 6-propionate and serine 45 and the absence of hydrogen bonds between 7-propionate and globin side chains in soybean LbCO.

Acknowledgment. This work was supported by Grant DK34909 from the National Institutes of Health. R.B. acknowledges a scholarship from the Swiss National Science Foundation.

(33) (a) Elber, R.; Karplus, M. *J. Am. Chem. Soc.* **1990**, *112*, 9161–9175. (b) Czerminski, R.; Elber, R. *Proteins: Struct., Funct. Genet.* **1991**, *10*, 70–80. (c) Stetzkowski, F.; Banerjee, R.; Marden, M.; Beece, D.; Bowne, S. F.; Doster, W.; Eisenstein, L.; Frauenfelder, H.; Reinisch, L.; Shyamsunder, E.; Jung, C. *J. Biol. Chem.* **1985**, *260*, 8803–8809.